IN SITU STRESS MEASUREMENTS AND FIELD VERIFICATION IN THE HSUEHSHAN TUNNEL

Chi-Wen YU[1] and Jin-Ching CHERN[2]

ABSTRACT

Hydraulic-fracturing stress measurements were conducted at planned sites of ventilation shaft 1 and shaft 2 of the Hsuehshan Tunnel during its basic design phase. In situ stress ratios, K_H (σ_H/σ_v) and Kh (σ_H/σ_v), were estimated to be on the order of 1.1 and 0.6 respectively. The general direction of H is N30°E, approximately perpendicular to the tunnel route. This data is also considered to be consistent with the extensional stress regimes found in Northeastern Taiwan. In this paper, the monitored data of the tunnel roof settlement and convergence during the construction phase were used to back calculate the in situ stress conditions, and then compared with the measured values. It was found that many back calculated tunnel sections of the various geological formations showed their KH values to be about 1.1 to 1.2. These results were quite consistent with the measured data.

Keywords: Hydraulic-fracturing, In situ stress, monitored data, back-calculated

INTRODUCTION

High stress conditions were expected in the route selection and design phases of Hsuehshan Tunnel. Therefore, during the basic design stage, the in situ stress measurements using hydraulic-fracturing techniques were conducted to evaluate the significance of in situ stresses which might impose on the tunnel construction (Chang and Cheng, 1992). The hydraulic-fracturing technique is one of the most widely accepted in situ stress determination methods for rock strata. The method utilizes the measurement of the pressure required to initiate and reopen fractures in a selected section of a borehole and the impression-taking of the fracturing plane to determine the magnitudes and orientation of the in situ rock stresses (ISRM, 1987).

The geologic profile along the tunnel route is shown in Fig. 1. The lithological changes are frequent and many major folds and faults were encountered in the tunneling process. The maximum overburden could have reached 700 m and in some tunnel sections the over-stressed rock mass causing stability problems was anticipated. Hydraulic-fracturing stress measurements had been conducted at the sites of planned ventilation shaft no.1 and shaft no.2. The test setups of the hydraulic-fracturing stress measurements in the Hsuehshan Tunnel are shown in Fig. 2.

Drilling at shaft 1 (PH-19, N2757898, E322393) was sunk to a depth of 268 m and at shaft 2 (PH-20, N2755027, E325364) to 257 m in order to eliminate topographic effect. Location plans of the tunnel route and the above-mentioned boreholes are shown in Fig. 3. A 3-D view, which exhibits the relief of the topography of the tunnel project area is shown in Fig. 4. The measurements were initially proposed to be conducted at all 3 shaft locations. However, due to the inferior geological conditions encountered in shaft no.3 (PH-29, N2752126, E327560), the measurements had to be abandoned (Sinotech Engineering Consultants, Inc. 1991). The results of all the in situ stress measurements are reviewed in the subsequent section and their significance to the tunnel construction and regional geologic setting are discussed.

CHARACTERISTICS OF IN SITU STRESSES

Stress Magnitudes

Table 1 shows the test results conducted at PH-19. At the test depths, the magnitudes of minimum horizontal stresses (σ_h) measured were in the range of 2.1 to 3.8 MPa, while the maximum horizontal stresses (σ_H) were in the range of 3.5 to 6.4 MPa. Table 2 shows the

1. Senior Research Engineer, Sinotech Engineering Consultants, Inc. E-mail : yu1014@sinotech.org.tw
2. Vice President, Sinotech Engineering Consultants, Inc. E-mail : jcchern@sinotech.org.tw

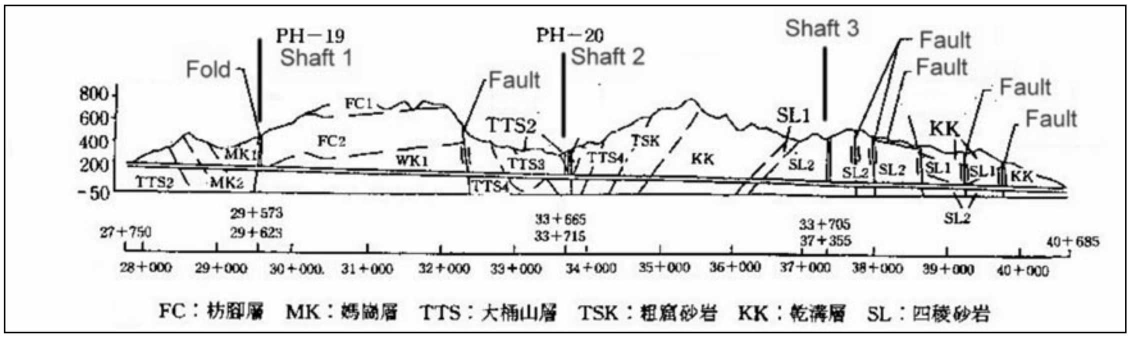

Fig. 1 Geologic Profile along the Tunnel Route

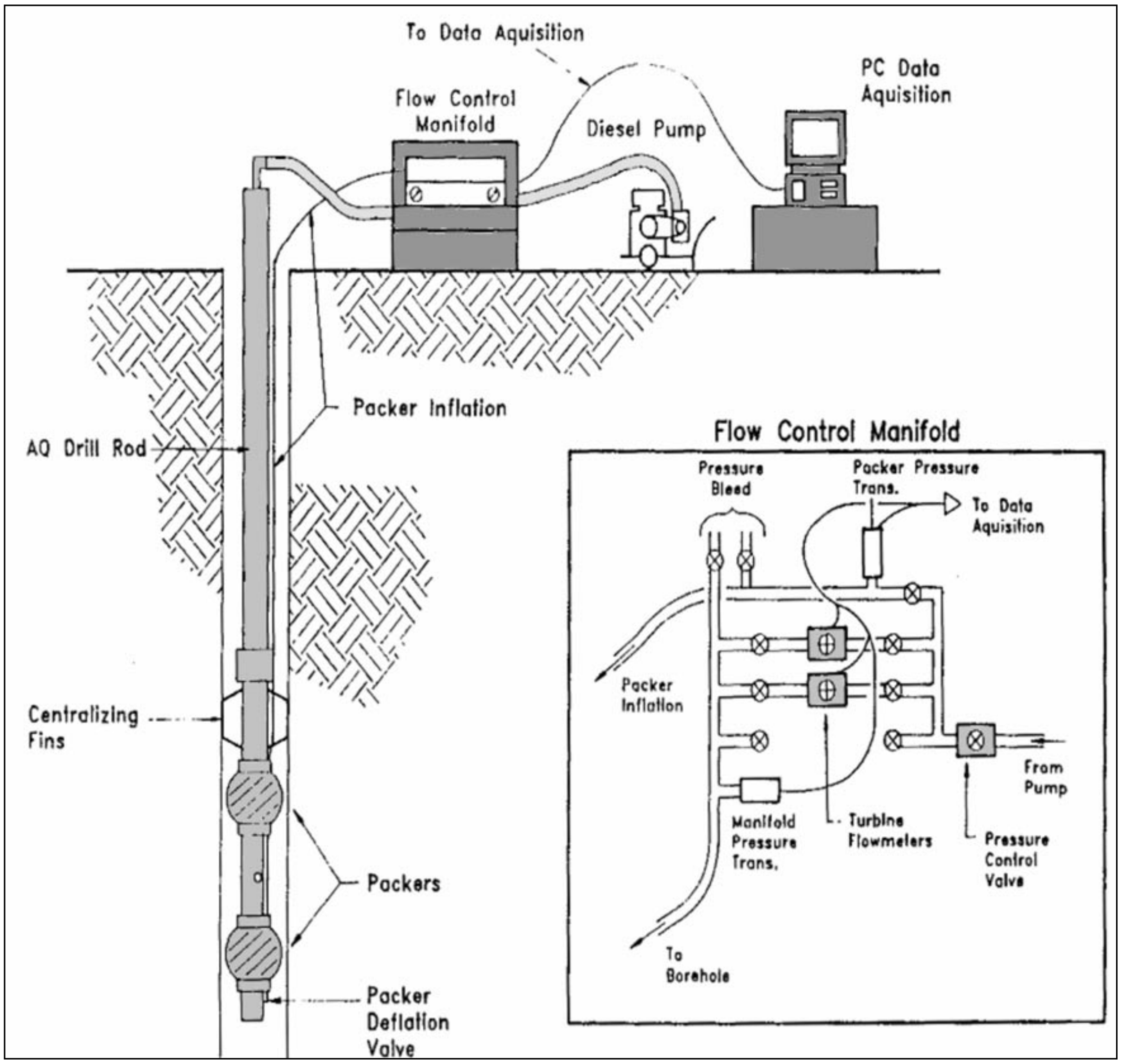

Fig. 2 Test Setup of Hydraulic-fracturing Stress Measurements, Hsuehshan Tunnel

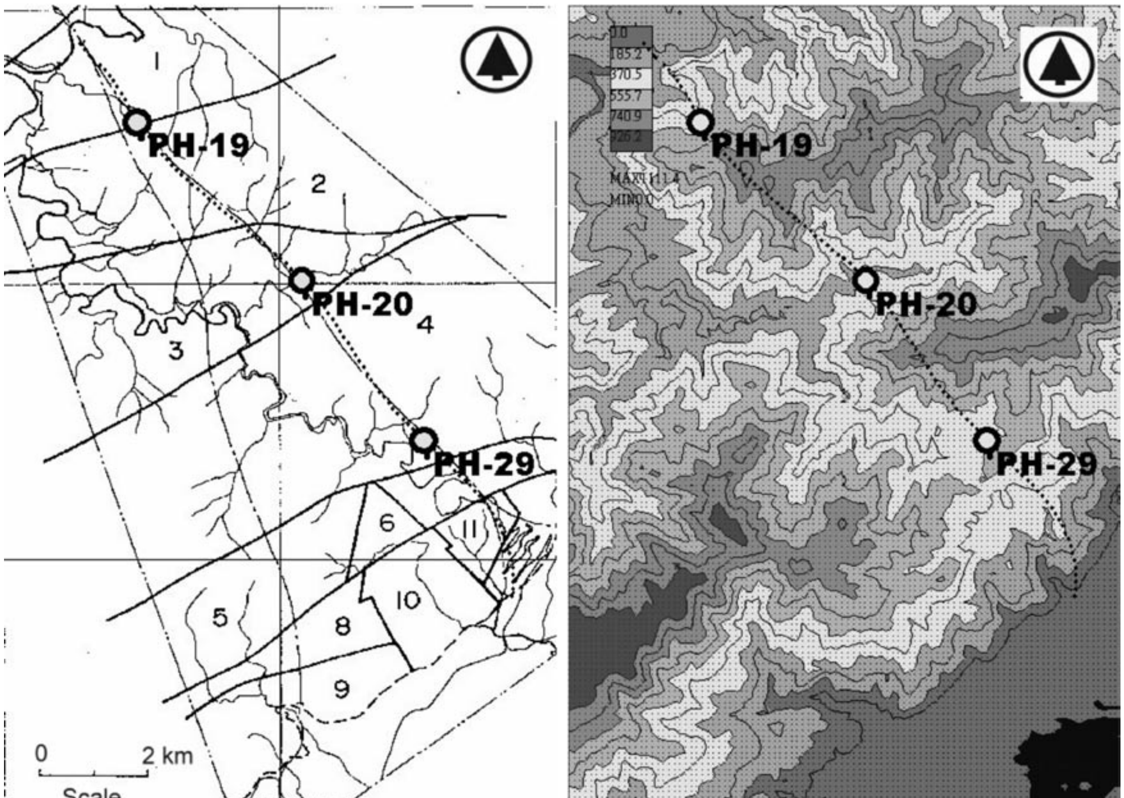

(a) With Geologic Zoning (1-10) (b) With Topography

Fig. 3 Location Plans of the Tunnel Route and Test Boreholes

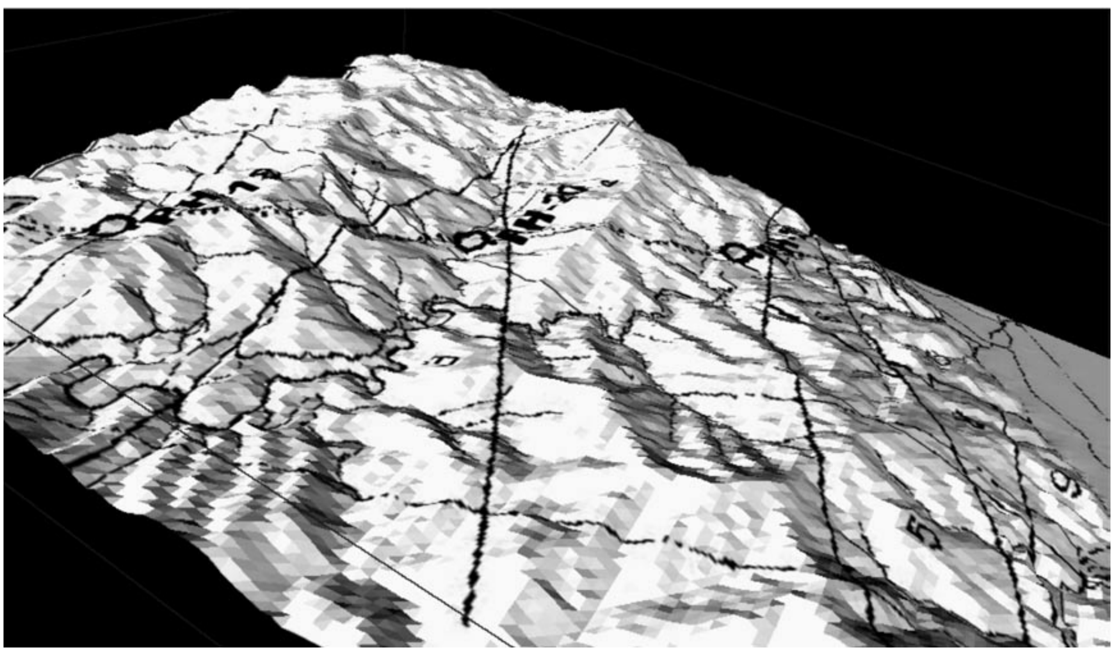

Fig. 4, 3-D view of the Topography of Tunnel Area

Table 1 Test Results at Borehole PH-19

Test No.	Top (M)	Bottom (M)	σ_H (MPa)	σ_h (MPa)	P_o (MPa)	σ_v (MPa)	Azimuth σ_H	Azimuth σ_h
PH19-01	156.1	156.9	4.3	2.7	1.5	3.8	32	122
PH19-02	160.1	160.9	5.7	3.4	1.6	3.9	41	131
PH19-03	168.1	168.9	-	-	1.7	4.1	-	-
PH19-04	169.1	169.9	-	-	1.7	4.2	-	-
PH19-05	181.7	182.5	6.1	3.8	1.8	4.5	24	114
PH19-06	212.4	213.2	3.5	2.1	2.1	5.2	-	-
PH19-07	213.5	214.3	4.3	2.2	2.1	5.2	4	94
PH19-08	232.1	232.9	6.4	3.7	2.3	5.7	-	-
PH19-09	250.2	251.0	4.6	2.9	2.5	6.1	14	104
PH19-10	258.1	258.9	-	-	2.5	6.3	-	-
PH19-11	265.9	266.7	-	2.7	2.6	6.5	-	-
PH19-12	267.0	267.8	6.1	2.9	2.6	6.6	108	18

Table 2 Test Results at Borehole PH-20

Test No.	Top (M)	Bottom (M)	σ_H (MPa)	σ_h (MPa)	P_o (MPa)	σ_v (MPa)	Azimuth σ_H	Azimuth σ_h
PH20-01	134.1	134.9	-	2.0	1.3	3.3	-	-
PH20-02	136.2	137.0	4.3	2.2	1.3	3.3	11	101
PH20-03	137.2	138.0	3.4	1.9	1.3	3.4	31	121
PH20-04	143.2	144.0	3.2	1.8	1.4	3.5	13	103
PH20-16	151.2	152.0	3.5	1.9	1.5	3.7	-	-
PH20-15	169.2	170.0	3.8	1.9	1.7	4.2	46	136
PH20-14	187.5	188.3	3.9	2.2	1.8	4.6	-	-
PH20-13	197.2	198.0	-	2.3	1.9	4.8	-	-
PH20-09	201.0	201.8	4.8	2.4	2.0	4.9	-	-
PH20-10	213.0	213.8	6.3	3.3	2.1	5.2	50	140
PH20-12	219.4	220.2	6.1	3.4	2.2	5.4	-	-
PH20-11	234.0	234.8	5.0	2.6	2.3	5.7	53	143
PH20-08	236.7	237.5	6.2	3.7	2.3	5.8	23	113
PH20-07	238.2	239.0	7.1	3.8	2.3	5.8	65	155
PH20-06	241.3	242.1	6.2	3.8	2.4	5.9	-	-
PH20-05	243.3	244.1	8.2	4.2	2.4	6.0	82	171
PH20-20	246.9	247.7	8.2	4.2	2.4	6.1	148	58
PH20-19	250.4	251.2	-	3.2	2.5	6.1	-	-
PH20-18	252.5	253.3	7.2	3.7	2.5	6.2	150	60
PH20-17	256.6	257.4	-	-	2.5	6.3	-	-

test results conducted at PH-20. The magnitudes of minimum horizontal stresses (σ_h) measured were in the range of 1.8 to 4.2 MPa, while the maximum horizontal stresses (σ_H) were in the range of 3.2 to 8.2 MPa.

Plots of test depths vs. results of the stress magnitude for PH-19 and PH-20 are shown in Fig. 5 and Fig. 6, respectively. The lithostatic and hydrostatic gradients are also shown for reference. The stress values are widely scattered especially those of the maximum stresses in

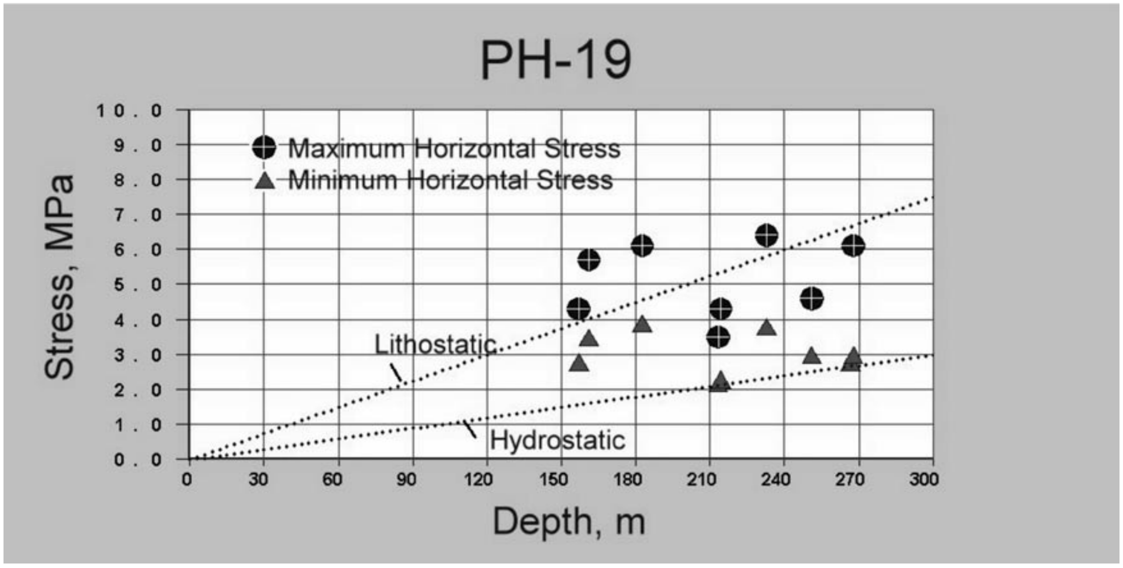

Fig. 5 Plots of Stress Magnitudes with Depths, Test of PH-19

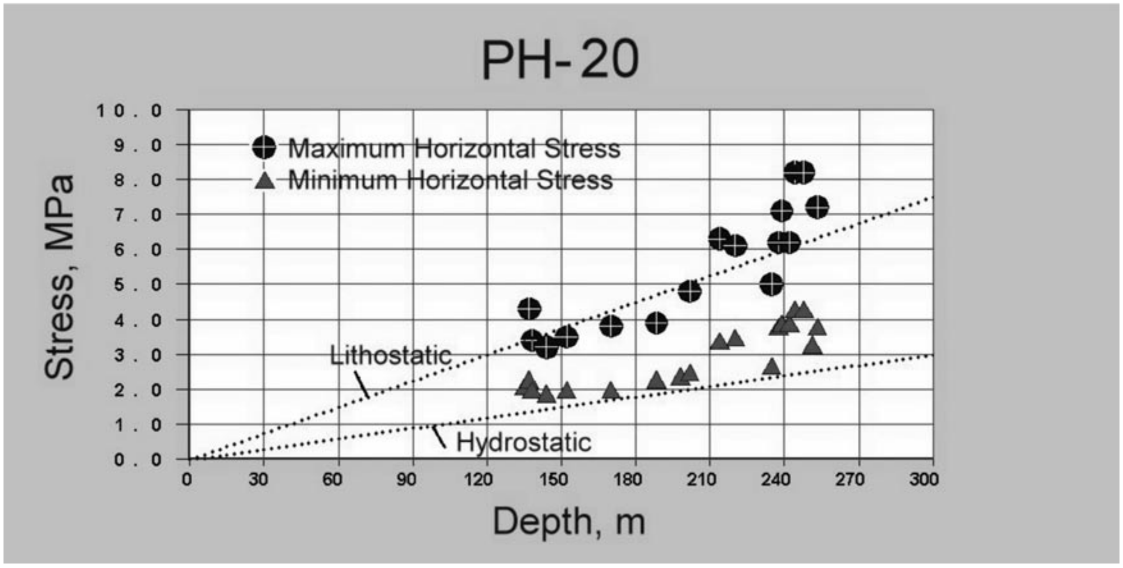

Fig. 6 Plots of Stress Magnitudes with Depths, Test of PH-20

PH-19, but follow in general the lithostatic trend. The poor correlation of stress results reflects the mechanical heterogeneity of the sedimentary rock layers. The lithologic variability is less in PH-19 than in PH-20. All of the test zones in PH-20 were logged as siltstones, although some contained clasts or thin interbeds of sandstone. This relative homogeneity may have been the source of the consistency of the stress results over the length of the borehole (Golder Associates, 1999).

Stress Orientation

The orientation of the stresses was determined from the orientation of the hydraulic-fractures in the boreholes. Examples of taking fracture impressions are shown in Fig. 7. The maximum stress direction (σ_H) is quite consistent over PH-19 and the upper 220 m of PH-20. The direction of the fractures is generally N23 E over PH-19 and N32 E to a depth of 237 m in PH-20. Below 237 m in PH-20, the fracture azimuth rotates from a northeast orientation to a northwest orientation. The average of the three deepest impressions in PH-20 is N126 E (N54 W), which is about a ninety degree rotation from the shallower test results and may represent a transition from one stress regime to another. The average direction of σ_H is estimated as running in a direction of N30 E, approximately perpendicular to the tunnel route. Measurements of the stress orientations against depths are shown in Fig. 8.

Stress Ratio

The vertical stress (σ_v) is normally assumed to be identical to the overburden stress. The in situ stress ratio K is defined as the horizontal stress divided by the vertical stress. As a consequence, $K_H = \sigma_H / \sigma_v$ and $K_h = \sigma_h / \sigma_v$. From the results shown in Fig. 5 and Fig. 6, it was found that a lower bound for the minimum stress is approximately hydrostatic, and a maximum stress is approximately lithostatic. As shown in Fig. 9, the curve-fitting processes of all these test data gives a K_H value on the order of 1.1, and a K_h value of 0.6, respectively.

Numerical Simulation of Stress Variations at Tunnel Routes

Changes in stress gradients can be estimated at PH-19 and PH-20. To examine the stress conditions in between these 2 shaft locations, the 2-D numerical finite difference code FLAC was used to analyze the potential stress variation on account of geologic zoning, topological and structural interference. Fig. 10 shows the geologic zoning for stress variation analysis between PH-19 and PH-20. It can be noted that the analyzed domain was truncated by a major fault (Chern and Yu, 1994).

Stress gradients estimated from PH-19 and PH-20 were adopted as the stress boundary inputs for the analysis. Results of stress variation analysis are shown in Fig. 11. Fig. 11(a) shows the vertical stress contour along the tunnel profile, and Fig. 11(b) the horizontal stress. As shown in the figure, the equal stress lines are more or less affected by the topological as well as lithlogical changes. However, the major influences come from the existence of a fault zone where the vertical stress is very different from the overburden stress. The horizontal stress is basically not affected by the existing fault.

ASSESSMENT OF IN SITU STRESSES DURING CONSTRUCTION

Back Calculation of Monitored Data

More than ten tunnel sections with monitored data through various geological formations at the westbound main tube (WB) were selected, and back-calculations using FLAC3D were conducted to obtain the rock mass parameters such as strength, deformability and K values. (Sinotech Engineering Consultants, Ltd., 2004). The results of the back calculation for these tunnel sections are outlined in Table 3.

Back-calculated K_H

Basically, the back analysis used the monitored data of the tunnel roof settlement and convergence during the construction phase under trial and error approaches. The in situ stress conditions of each analyzed section are denoted by K values, where the overburden stress was taken to be σv, $\sigma_H = K_H\sigma_v$ and $\sigma_h = K_h\sigma_v$. It was found that many back calculated tunnel sections of various geological formations showed their K_H values of 1.1 to 1.2. These results are consistent with the measured data of the hydraulic fracturing test.

Fig. 12 shows the monitored data of the tunnel roof settlement plotted against horizontal convergence of the selected tunnel sections. The data are widely scattered but follow in general the trend of (1 : 2) which represents the tunnel deformation when K values in the section of advancing face equals unity. The poor correlation may reflect the influence of rock mass heterogeneity or the existence of adjacent tunnels.

DISCUSSIONS

Geological Setting of Tunnel Area

Taiwan is located at the boundary between the Philippine Sea Plate (PSP) and the continental margin of the Eurasian Plate (EUP). The Taiwan orogen is regarded as the result of the active collision of these plates. In Northeastern Taiwan, the PSP is subducting beneath the rifted EUP Margin (Ryukyu Margin) along the Ryukyu Trench and the stress pattern is regarded as extensional due to the back-arc opening of the Okinawa Trough (Tsai, 1983; Lee, 1986; Font et al., 2003). The geological setting of this complex plate junction is illustrated in Fig. 13 and Fig. 14.

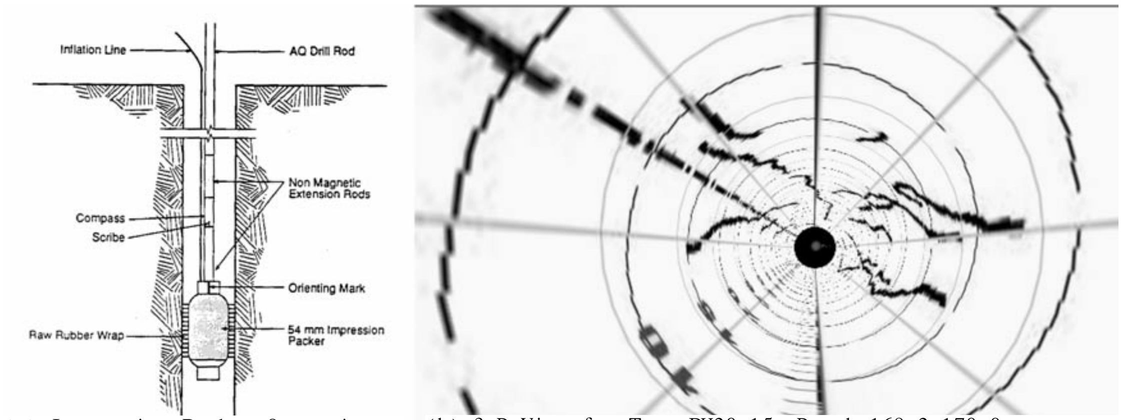

(a) Impression Packer Operation (b) 3-D View for Test PH20-15, Depth 169.2-170.0 m

Fig. 7 Stress Orientation Taken by Impression Packer

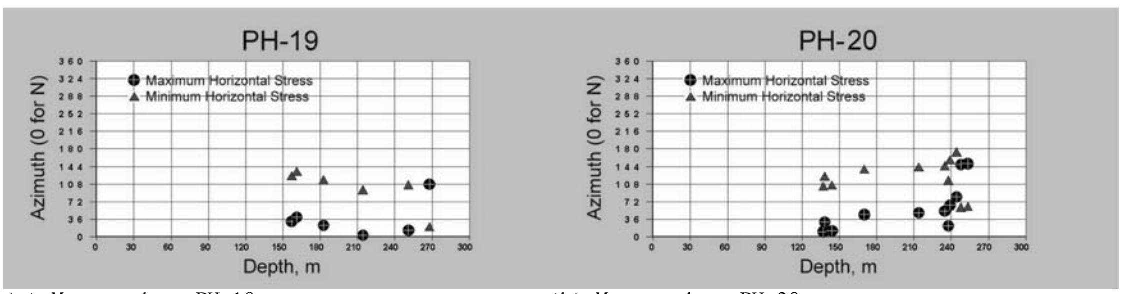

(a) Measured at PH-19 (b) Measured at PH-20

Fig. 8 Stress Orientation Measurements

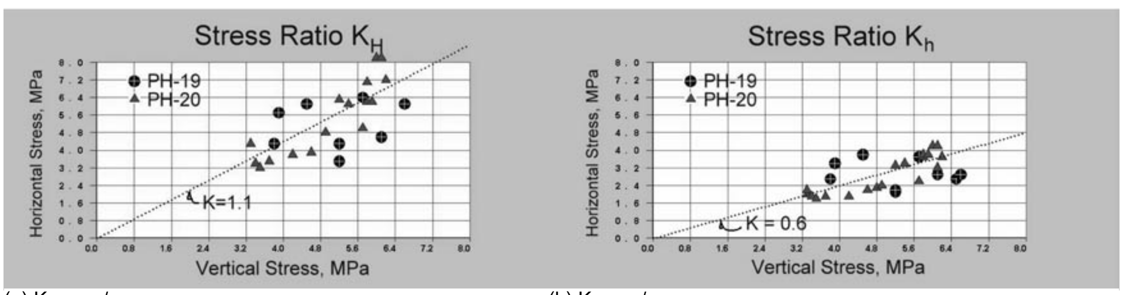

(a) $K_H = \sigma_H / \sigma_v$ (b) $K_h = \sigma_h / \sigma_v$

Fig. 9 Stress Ratio K

Tunnel Behavior

The back-arc opening of the Okinawa Trough is believed to extend its effect all the way to the Ilan Plain, a delta area located in Northeastern Taiwan. As a consequence, the Tunnel area is affected by this extensional stress regime. In the Tunnel area, the measured magnitude of the average K_h is 0.6, the average K_H about 1.1, and the direction of σ_H is approximately N30 E running approximately perpendicular to the tunnel route with a bearing of about 140 . Therefore the extensional stress conditions along the tunnel advancing direction are expected.

This extensional stress regime also explains the reason why many of the rock masses adjacent to the

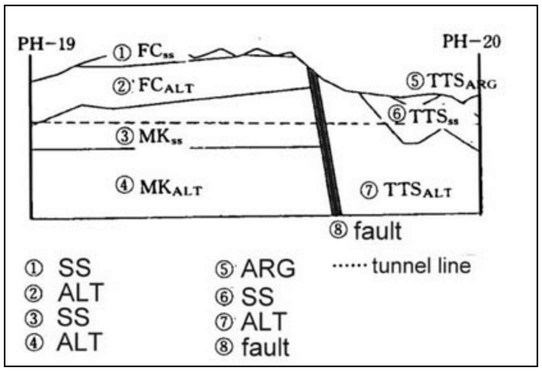

Fig. 10 Geologic Zoning of Stress Variation Analysis between PH-19 and PH-20

large normal faults cause problems when tunneling the eastern part of the tunnel through the Szeleng Formation. In these sections, many unstable roof conditions existed and water inflows were severe.

The orientations and magnitudes of the in situ stresses obtained are regarded as quite consistent with the stress regimes associated with the regional geologic setting in Northeastern Taiwan. Fig.14 (b) shows the overall stress patterns around the tunnel project area.

CONCLUSIONS

Hydraulic-fracturing techniques were used to determine the in situ stresses along the two shaft locations of the Hsuehshan Tunnel. In situ stress ratios, K_H ($\sigma_H/\sigma v$) and Kh ($\sigma_h/\sigma v$), were estimated to be on the order of 1.1 and 0.6 respectively. The average direction of σ_H is N30E, approximately perpendicular to the tunnel route with a bearing of about 140 .

The monitored data of the tunnel roof settlement and convergence during the construction phase were used to back calculate the in situ stress conditions. Comparing the calculated K_H values with the measured values, it was found that many back calculated tunnel sections of various geological formations showed K_H values that were about 1.1 to 1.2. These results are quite consistent with the measured data.

The data obtained was proven to be very helpful in the design and construction of the tunnel project. These data not only provided valuable references to the design and construction plan, but also gave evidence in the explanation of the extensional stress regimes in the geologic setting of Northeastern Taiwan.

REFERENCES

* Tsai, Y. B. (1983), "Status of earthquake prediction research in Taiwan," Bull. Inst. Earth Sci. Academia Sinica, Vol. 3, 1-26.
* Lee, C. T. (1986), "Analysis of geo-technical stresses and study of the effects of the migration of paleo-stresses due to arc-continent collision in northern Taiwan," PHD Thesis, National Taiwan University.
* I. S. R. M. (1987), "Suggested methods for rock stress determination," Int. Journal of Rock Mech. Min. Sci. & Geomech. Abstr., Vol. 24, No.1.
* Golder Associates Inc. (1991), "Report of hydraulic-fracturing stress measurements for the Pinglin Tunnel."
* Sinotech Engineering Consultants, Inc. (1991), "Basic design phase evaluation report of geo-mechanical test and investigation, Pinglin-Touchen section, Taipei-Ilan Expressway."
* Chang, W. C., Cheng, W. L. (1992), "In situ stress measurements and their application for tunnel design in northern Taiwan," Journal of ISRM Symposium: Eurock 92,, Chester, UK.
* Chern, J. C., Yu, C. W. (1994), "In situ stress determination using hydraulic-fracturing technique

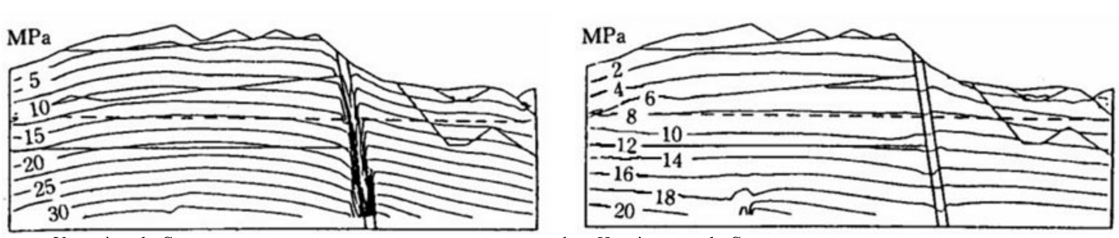

(a) Vertical Stress (b) Horizontal Stress

Fig. 11 Results of Stress Variation Analysis (a) Vertical Stress, (b) Horizontal Stress

TABLE 3. K Values Back Calculated by Monitoring Data

NO	TUNNEL ID	STATION (M)	ROCK FORMATION	RS (MM)	H1 (MM)	X (M)	RMR	OVB (M)	K
1	“WB”	28069	“TTS”	2	2.5	6.5	45	250	1.2
2	“WB”	28255	“TTS”	2	-1	25	44	210	1.2
3	“WB”	28660	“TTS”	10	5	2.5	45	180	1.2
4	“WB”	28960	“MK”	20	60	6	30	250	1.1
5	“WB”	29281	“MK”	9	3	5	55	365	1.1
6	“WB”	29710	“FC”	6	9	4	35	590	1.1
7	“WB”	30300	“MK”	1	3	14	52	630	1.1
8	“WB”	31200	“MK”	3	9	9.5	35	650	1.1
9	“WB”	33151	“TTS”	12	21	3.3	20	230	1.2
10	“WB”	34400	“TSK”	3	3	4	58	540	1.1
11	“WB”	34500	“TSK”	3	5	6.5	48	580	1.1
12	“WB”	35721	“KK”	2	3	13	48	500	1.1
13	“WB”	36015	“KK”	3	7	9.5	28	470	1.1
14	“WB”	36096	“KK”	8	11	4.5	35	450	1.1
15	“WB”	36996	“SL”	8	22	4.5	18	440	1.1
16	“WB”	37098	“SL”	9	21	6	10	480	1.1
17	“WB”	37875	“SL”	2	4	3	40	370	1.1
18	“WB”	38131	“SL”	11	8	3	38	370	1.1

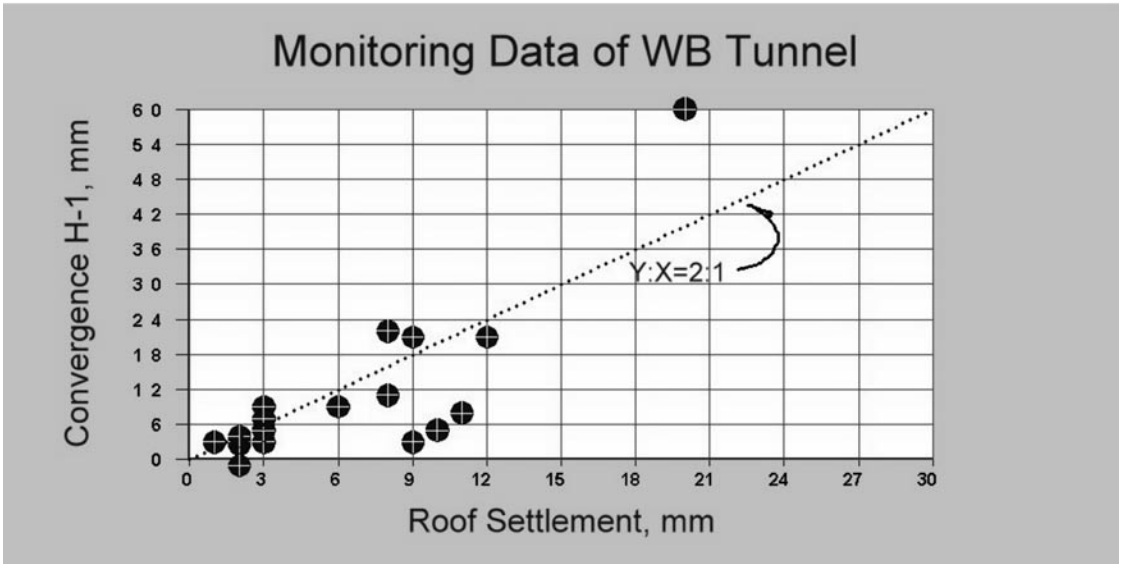

Fig. 12 Comparison of Monitoring Data by Roof Settlement and Horizontal Convergence

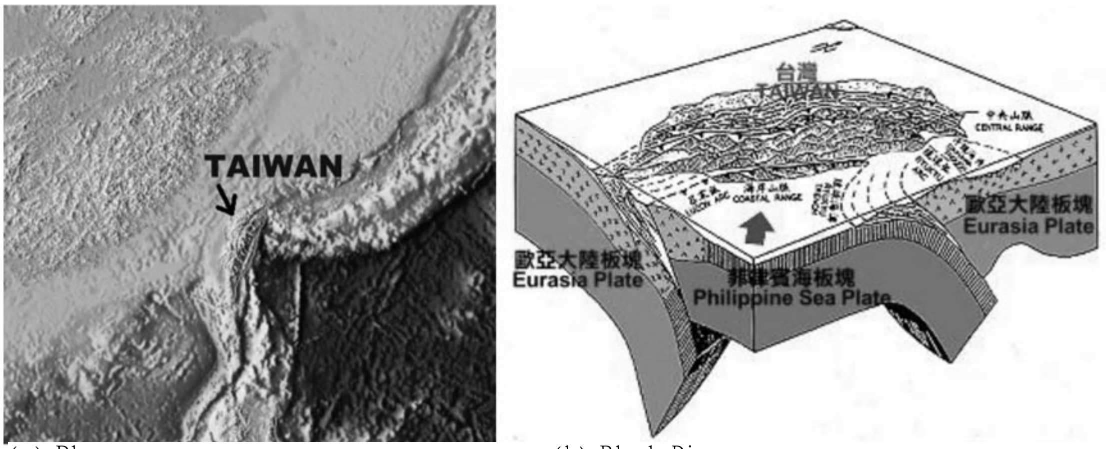

(a) Plan (b) Block Diagram

Fig. 13 Geological Setting of Taiwan

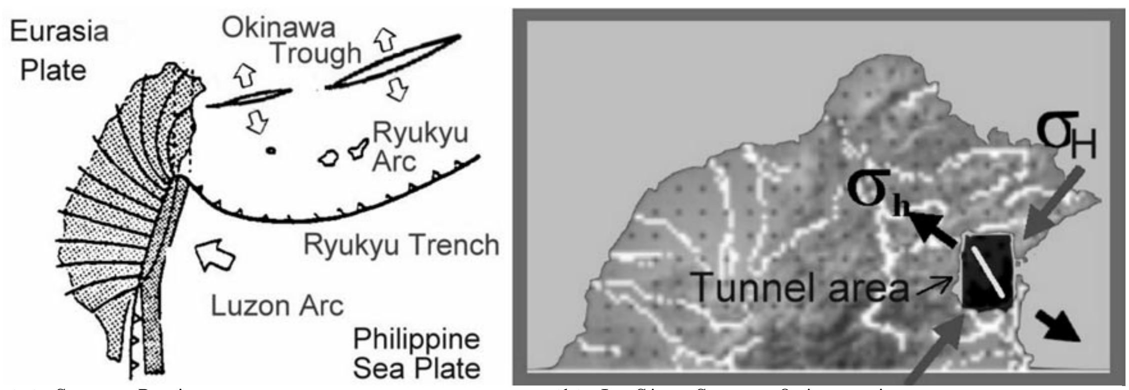

(a) Stress Regime (b) In Situ Stress Orientation

Fig. 14 Stress Regime of the Hsuehshan Tunnel Area

along Pinglin Tunnel routes," Journal of Sino-geotechnics, No.46, 35-46.

* Font, Y., Kao, H., Liu, C. S., Chiao, L. Y. (2003), "A comprehensive 3D seismic velocity model for the eastern Taiwan-southernmost Ryukyu region," Journal of Terrestrial, Atmosphericand Oceanic Sciences, Vol. 14, No.2, 159-182.

* Sinotech Engineering Consultants, Ltd. (2004), "Final evaluation report of geologic investigations of Pilot Tunnel, Hsuehshan Tunnel."